



Location of greenspace matters: a new approach to investigating the effect of the greenspace spatial pattern on urban heat environment

Guanhua Guo · Zhifeng Wu · Zheng Cao · Yingbiao Chen · Zihao Zheng

Received: 17 June 2020 / Accepted: 1 March 2021 / Published online: 23 March 2021
© The Author(s), under exclusive licence to Springer Nature B.V. 2021

Abstract

Context Although many prior efforts have found that both spatial composition and configuration of greenspaces significantly affect the urban heat environment globally, the spatially heterogeneous effects of greenspace spatial patterns on the urban heat environment remain poorly understood for urban spaces.

Objectives We proposed a spatially explicit approach to investigate the spatially heterogeneous cooling effects of greenspaces and map the relative contributions of the greenspace spatial patterns to the characterization of the urban heat environment.

Methods The proposed approach integrated the best subsets regression method, geographically weighted regression (GWR), and hierarchical partitioning analysis. Two cities in southeastern China were selected to

test our model. Landsat 5 image obtained in the summer was used to estimate the land surface temperature (LST) and greenspace spatial patterns were extracted from 0.5-m aerial images.

Results The results revealed that LST of Guangzhou can be well predicted by the percent cover (PER), the number of patches (NP), the area-weighted mean of the patch area (AREA_AM), and the area-weighted mean of the perimeter-area fractal dimension (FRAC_MN), while that of Shenzhen can be predicted by PER, NP, AREA_AM and the mean of the related circumscribing circle (CIRCLE_MN). The inclusion of additional landscape metrics did not yield significantly higher accuracies. The dominant landscape metrics of greenspace that determine the LST varied spatially across the two cities, with the PER accounting for the greatest variation.

Conclusion The results of our work demonstrate that the location of greenspace is a significant factor affecting the urban heat environment. The proposed approach provides a new understanding of the interaction between the greenspace spatial patterns and urban heat environments, providing useful information for tailoring greenspace planning policies for specific local sites.

Supplementary Information The online version contains supplementary material available at <https://doi.org/10.1007/s10980-021-01230-w>.

G. Guo · Z. Wu (✉) · Z. Cao · Y. Chen
School of Geography and Remote Sensing, Guangzhou University, Guangzhou 510006, China
e-mail: zfwu@gzhu.edu.cn

G. Guo · Z. Wu · Z. Cao
Southern Marine Science and Engineering Guangdong Laboratory, Guangzhou 511458, China

Z. Zheng
Department of Land, Environment, Agriculture and Forestry, University of Padova, 35020 Padova, Italy

Keywords Spatially heterogeneous approach · Urban heat environment · Greenspace spatial pattern · Dominant landscape metrics · Land surface temperature

Introduction

The area of urban regions is expected to increase by 1.2 million km² by 2030, which is nearly triple the global urban area in 2000 (Seto et al. 2012). Although urbanization has significantly improved the socio-economic well-being of urban residents, it can potentially threaten a range of ecosystem services and biodiversity features (Seto et al. 2012; Peng et al. 2017; Pickard et al. 2017). The urban heat island (UHI) effect, which describes the atmospheric phenomenon of increased surface and air temperatures compared with the surrounding rural areas (Oke 1973; Voogt and Oke 2003), is one of the most recognizable environmental problems caused by urbanization. Specifically, the transformation from natural and semi-natural (e.g., forest, farmland, water body) ecosystems to the artificial surface (e.g., impervious surface) primarily contributed to the hotter environment in core urban areas. The increased temperatures may result in a broad range of unintended and negative consequences (Wang 2009; Gabriel and Endlicher 2011; Skelhorn et al. 2016; Xu et al. 2016; Wang et al. 2018b). Aware of these impacts, research communities consisting of different professional fields have made great efforts to obtain scientific knowledge of the UHI, seeking technologies and strategies for urban planners to create a comfortable thermal environment in urban regions.

Microclimates within densely populated cities are unique from regional patterns owing to the various environmental configurations and functional uses, resulting in different environmental variables exerting varying degrees of influence on the UHI (Wong et al. 2016). Although a considerable amount of recent effort has been applied to explore the UHI mechanisms (Li et al. 2016; Zhou et al. 2017b; Peng et al. 2018; Liu et al. 2018b; Ziter et al. 2019), we still only have a minimal understanding of how landscape patterns in urban areas impact the LST at different sites. Most of the previous efforts utilized global statistical methods, assuming that the relationships between the urban heat environment and corresponding driving factors were constant over the entire study area. Thus, these studies may neglect the issues of spatial non-stationarity, regarded as the intrinsic properties of the urban ecosystem (Wu and David 2002; Foody 2003; Li et al. 2010; Su et al. 2012). In the investigation of this mechanism, spatial non-

stationarity relationships should be considered with a local regression technique, and site-specific optimized mitigation strategies should be provided for contrasting environmental configurations. Ivajnsič et al. (2014) stated that the data related to geographical patterns and processes in nature are always georeferenced, which means that their measurements are defined as local non-stationary explanatory variables, rather than by universal physical laws. Additionally, some recent work has indicated that the constant internal variation of urban areas has not been considered (Wang et al. 2018a; Zhou et al. 2019). From this perspective, an interesting question emerges: how can we investigate spatially explicit influences of a regional urban heat environment?

Greenspace refers to the landscape that comprises vegetation and is associated with natural elements (Taylor and Hochuli 2017), providing a wide range of benefits for dwellers, including UHI mitigation by intercepting solar radiation with shading surfaces and reducing the surrounding temperature through evapotranspiration (Arnfield 2003; Greene and Kedron 2018). Hence, the impact of greenspace spatial patterns on UHI has been intensively studied, especially with thermal infrared images that are used to derive the LST (Li et al. 2012; Maimaitiyiming et al. 2014; Sun and Chen 2017; Zhou et al. 2017b; Chun and Guldmann 2018; Greene and Kedron 2018; Guo et al. 2019). It is known that increasing the percentage of greenspace may significantly produce a cooler environment. However, such spaces in densely populated cities are limited, leading to increased interest in the optimization of the greenspace spatial configuration to maximize its ability to mitigate UHI (Zhang et al. 2017; Zhou et al. 2017b; Guo et al. 2019). Zhou et al. (2017b) and Guo et al. (2019) found that the consideration of whether spatial composition or spatial configuration is more important was inconsistent among the studies, primarily because of the different urban planning contexts and local climates of the various study areas. Landscape patterns are characterized by spatial heterogeneity in ecological systems (Pickett and Cadenasso 1995; Wu and David 2002; Zhou et al. 2017a), especially in core urban areas. Consequently, the spatial pattern of the UHI, as well as its deriving influence, vary with the local site conditions. In this context, other practical questions arise: Is greenspace composition or configuration more important in determining the LST at the local scale? What

are the dominant landscape metrics for a specific location in heterogeneous inner cities?

In this study, we developed an approach by integrating the best subset regression, geographically weighted regression (GWR), and hierarchical partitioning analysis, to detect the representative landscape metrics of greenspaces that determine the LST and map the contributions of greenspace to the urban heat environment across cities. This idea is based on the assumption that the LST pattern and its influence in urban areas are highly heterogeneous. Unlike previous studies that only treat the UHI mechanism as a single unit, our method further employs the spatial heterogeneity of site-specific information. The success of this technique is derived from two aspects: (1) representative landscape metrics of greenspaces may not be consistent in different cities; thus, we potentially need to determine the specific landscape metrics according to a given study area. This issue can be overcome based on a metrics detection algorithm that integrates stepwise regression and best subsets regression. (2) The impact of the greenspace spatial pattern on the LST varies with local site conditions, leading to dominant landscape metrics that tend to be spatially explicit. Thus, we proposed a local regression technique by integrating GWR and hierarchical partitioning to solve this problem. We tested the proposition in two highly urbanized cities, Guangzhou and Shenzhen, in southeastern China, and attempted to address the aforementioned scientific questions.

Methodology

Study area

Guangzhou and Shenzhen in the Pearl River Delta (PRD) metropolitan region of southeastern China were chosen as the study area (Fig. 1). These cities are representative of many highly urbanized cities located in the subtropics and are characterized by hot and humid summers (Peng et al. 2018). Guangzhou is the capital city of Guangdong province, with a total area of 7434 km² and a population of approximately 14.49 million in 2018. Its GDP reached CNY ¥ 2.3 trillion in 2018, accounting for 20% of the GDP in Guangdong province. Shenzhen is a newer city than Guangzhou, serving as one of the four special economic zones established in China. The area of Shenzhen is greater

than 1996 km², with a population of 13.02 million and a GDP of CNY ¥ 2.4 trillion in 2018. Consequently, Guangzhou and Shenzhen have experienced extremely rapid urbanization and have become world cities. In this study, we focused on the highly urbanized areas of the two cities, as shown in Fig. 1b. The study area of Guangzhou was the central urban area consisting of the main highly urbanized districts of Guangzhou with 126 census tracts, covering approximately 1461.66 km². We selected western Shenzhen because it is the primary economic development growth engine of the city rather than including the eastern portion that serves as an eco-environmental protection area (Peng et al. 2018). These selected areas are characterized by greater development than other parts of the respective cities, and they can sufficiently represent the urban heat environment of rapidly urbanized cities.

Development of a new method

Step 1: LST and greenspace extraction

A cloud-free Landsat-5 image (path 122, row 44) acquired on June 1, 2011 was used to characterize the LST spatial distribution. The Landsat-5 image is a Level A product downloaded from the United States Geological Survey (<https://glovis.usgs.gov/>). The LST retrieval was accomplished in two steps (Qin et al. 2001; Peng et al. 2018; Guo et al. 2019): (1) the digital number (DN) of the thermal infrared band in the Landsat-5 image was converted to the radiation brightness temperature; (2) the actual LST was calculated from the radiation brightness temperature with the use of a mono-window algorithm. Finally, the LST data with 120 m spatial resolution was obtained.

The greenspace was mapped based on the aerial images with 0.5 m spatial resolution acquired in 2010. For classification, four classes were considered: greenspace, impervious surfaces, water bodies, and bare soil, with the use of an object-oriented classification approach using the eCognition Developer software (Definiens Imaging, Inc., Germany). The classification accuracy was examined based on a confusion matrix with more than 90 randomly selected points for each city. Finally, the overall classification accuracies of the greenspace were 93.23% and 92.16%, and the kappa coefficients were 0.89 and 0.86 for Guangzhou and Shenzhen, respectively (Fig. 1c, d).

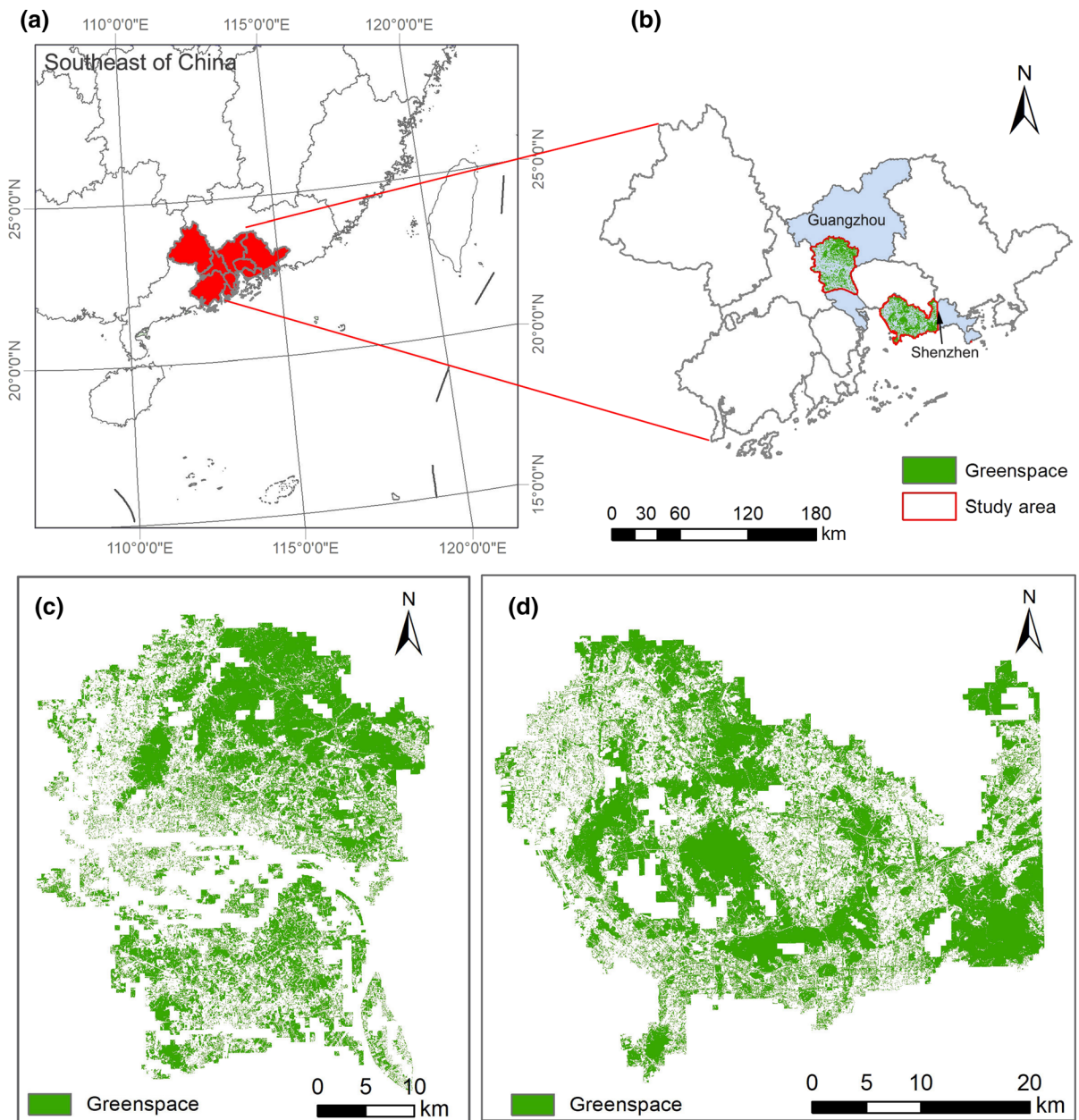
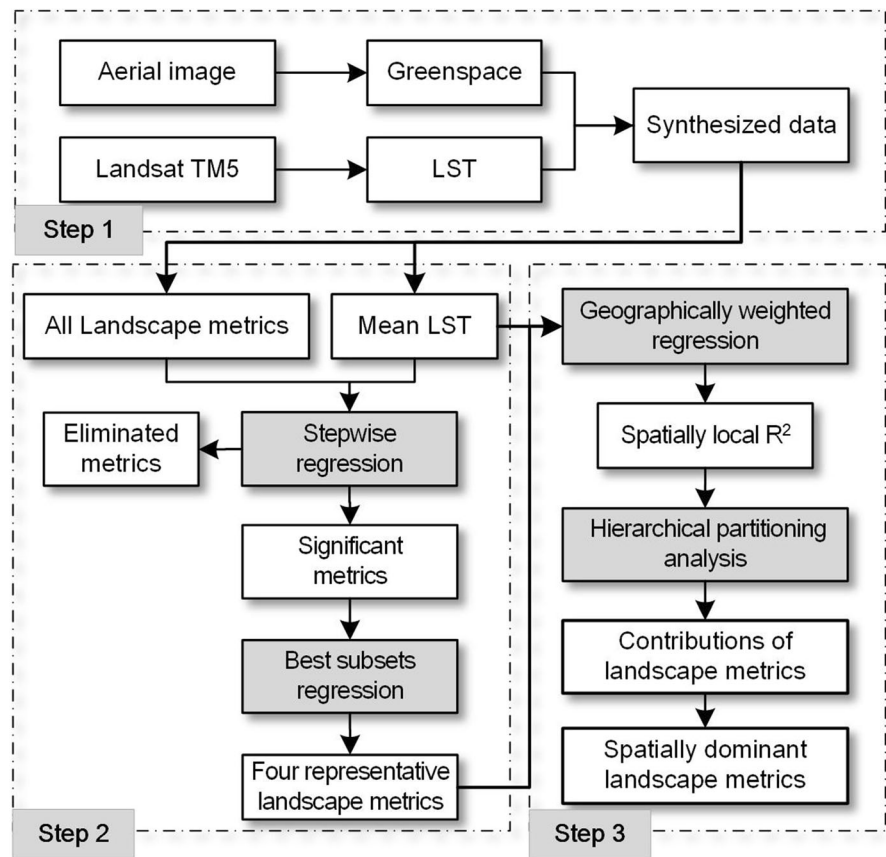


Fig. 1 **a** Location of the Pearl River Delta (PRD) metropolitan area in southeastern China, and **b** study areas in the cities of Guangzhou and Shenzhen. **c**, **d** show the spatial patterns of greenspace of the two cities

A $500\text{ m} \times 500\text{ m}$ fishnet layer was created to present the size of neighborhoods of the two cities and systematized the LST and greenspace spatially, thereby allowing the examination of the complex mechanism of the LST (Guo et al. 2016; Zhou et al. 2017b). For each block, the mean LST values were calculated based on zonal statistics as the response

variable, and the landscape metrics of greenspaces were the predictor variables. We focused on the terrestrial parts of the cities; the blocks containing water bodies were excluded from the statistical analyses. The total number of blocks was 4,336 and 4,430 for Guangzhou and Shenzhen, respectively (Fig. 2, step 1).

Fig. 2 Flowchart of the proposed approach

Step 2: identification of representative landscape metrics

Landscape metrics can effectively display the spatial composition and configuration of the land cover (Turner 2005; Zhou et al. 2011). They have been widely used to investigate greenspace landscape patterns and their impacts on the UHI (Li et al. 2013; Zhou et al. 2017b; Guo et al. 2019; Li and Zhou 2019). In previous studies, the selection of landscape metrics was based on principles such as interpretability, redundancy, and theoretical importance, but without an objective examination. Landscape metrics are often correlated (Liu et al. 2018a), causing multicollinearity when various metrics are included in the LST models. Moreover, different study areas were characterized by their distinct ecological contexts (Wu et al. 2015; Zhou et al. 2017b). Consequently, applying an objective method to determine the representative landscape metrics for a specific study area is an essential part of the investigation of

the complex relationships between greenspace landscape patterns and the LST.

In this study, a total of 27 landscape metrics at the class level were considered, including the commonly used metrics of patch density (PD), landscape shape index (LSI), and edge density (ED) and uncommonly used metrics, such as mean-related circumscribing circle distribution (CIRCLE_MN) and contiguity index (CONTIG_AM). These landscape metrics in each block were calculated using Fragstats 4.2 software (McGarigal et al. 2012). Their definition and calculated equation can be found in the user manual of the software. The “8-cell” rule was used to define the patch neighbors during the landscape metrics calculation.

The objective method for detecting representative landscape metrics includes two steps: stepwise regression followed by best subsets regression (Fig. 2, step 2). First, we employed the stepwise regression model to eliminate the non-significant landscape metrics of greenspaces, whereas those influencing landscape

metrics with no multicollinearity were found with a significance test at the 0.01 level. Second, we applied best subsets regression to consider all the possible combinations of influencing landscape metrics (Wang 2009; Peng et al. 2018). Considering all the influencing landscape metrics, the best subsets regression calculates and compares all possible models using a specified set of landscape metrics and then assesses the best-fitting models that contain only one landscape metric, two landscape metrics, and so on. The adjusted R^2 value was used as an indicator to define the goodness of fit for the model.

Step 3: detecting dominant landscape metrics spatially using an integrated method

After confirming the representative landscape metrics of greenspaces in determining the LST in step 2, we constructed an integrated method incorporating the GWR and hierarchical partitioning analysis to further map the relative contributions of the landscape metrics spatially (Fig. 3, step 3). First, we proposed a GWR model to perform the complex derivation of the influence on the LST by greenspace spatial patterns. GWR is a local regression technique with the ability to examine the effects of local spatial heterogeneity on complex relationships, which is a significant improvement over commonly used global regression analyses, such as the ordinary least squares (OLS) model (Brunsdon et al. 1996; Wang et al. 2008; Li et al. 2010; Van Donkelaar et al. 2015). The GWR model for the LST calculation can be expressed as

$$LST_i = \beta_0(u_i + v_i) + \beta_1(u_i + v_i)x_{i1} + \beta_2(u_i + v_i)x_{i2} + \dots + \beta_n(u_i + v_i)x_{in} + \varepsilon_i, \quad (1)$$

where LST_i is the actual LST values in the i -th block, u_i and v_i refer to the spatial location of the i -th block; x_{i1}, x_{i2}, x_{in} refer to the representative landscape metrics in the i -th block; β_0 denotes the intercept of the model; $\beta_1, \beta_2,$ and β_n are the slopes of the representative landscape metrics; and ε_i is the random error term at the i -th block. The GWR model created a spatial pattern of intercepts ($\beta_0(u_i + v_i)$), variable coefficients (e.g., $\beta_1(u_i + v_i)$), and a local R^2 to characterize the spatial non-stationarity, indicating that the impacts of the greenspace spatial patterns on the LST will vary with the local site conditions. Specifically, the bandwidths generalizing the optimal GWR were determined by a cross-validation method that produced the lowest root-mean-square prediction error.

Second, 2^n (n is the number of representative landscape metrics) possible GWR models were implemented to derive the local R^2 representing the effects causing the change in the LST by the landscape metrics of greenspaces across the study sites. Hierarchical partitioning, an excellent multidimensional environmental data analysis method (Mac Nally 2000; Peng et al. 2018; Guo et al. 2019), was utilized to identify the relative contribution of each selected landscape metric contained in the GWR models. These representative landscape metrics were sorted by their independent contributions in descending order to

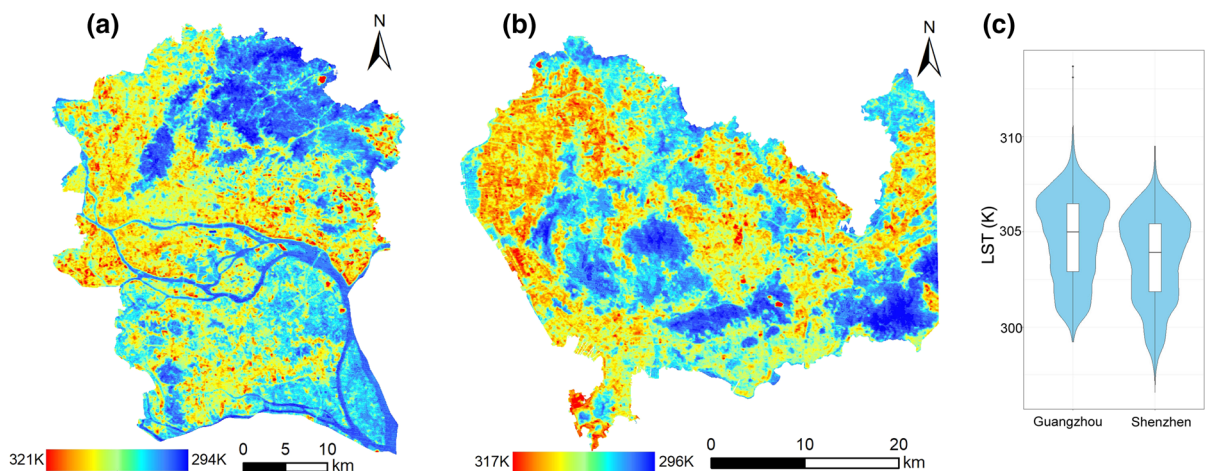


Fig. 3 Spatial pattern of LST in **a** Guangzhou, **b** Shenzhen, and **c** the statistical distribution of their values

detect the dominant landscape metrics (i.e., most powerful metrics) in determining the LST.

We also proposed an intensity dominance gap (IDG) term to quantify the dominance difference of the independent contribution between the most powerful landscape metric and the second most powerful landscape metric in each block:

$$IDG_i = IDGf_i - IDGs_i, \quad (2)$$

where, IDG_i , in %, is the dominance difference of the most powerful landscape metric in the i -th block, $IDGf_i$ and $IDGs_i$ are the independent contribution of the most powerful and second most powerful landscape metric in the i -th block, respectively.

Results

Spatial patterns of greenspace and LST

As shown in Table 1, greenspaces in Guangzhou and Shenzhen exhibited similar percent cover (PER) values but a significantly diverse spatial configuration. Approximately 52.86% of the land in Guangzhou and approximately 53.85% in Shenzhen were covered by greenspace. The PER of greenspace varied greatly across the urban regions for both cities (Fig. 1b). Taking Guangzhou as an example, the greenspace is more clustered with larger patch sizes in the northeast region. However, the greenspace is more scattered with fewer and smaller patches in the middle area. This is largely because these places are the most highly urbanized regions, covered by high-density buildings and institutions with absent vegetated landscapes. Regarding the spatial configuration, the patch density (PD) of the greenspace in Shenzhen was greater than that in Guangzhou with lower edge density (ED), suggesting that the greenspace in Shenzhen exhibited a greater number of patches with less complexity in

Table 1 Greenspace spatial patterns in the two cities

Cities	PER (%)	PD (/100 ha)	LPI (%)	ED (m/ha)
Guangzhou	52.86	71.12	7.71	546.08
Shenzhen	53.85	87.24	10.55	507.17

PER percent cover with unit of %, *PD* patch of density with unit of number per 100 hectares, *LPI* largest patch index with unit of %, *ED* edge density with unit of m/ha

shape. The largest patch index (LPI) was greater in Shenzhen, suggesting the existence of a larger greenspace patch.

The LST varied greatly across the urban areas for both cities, as shown in Fig. 3. Guangzhou produced a higher LST, ranging from 294 to 321 K, with a mean LST of 304.61 K. The LST in Shenzhen ranged from 296 to 317 K, with a mean of 303.57 K. It is evident from Fig. 3a and b that a thermal gradient progressed from the city center to the countryside. Many LST hot spots can be visually identified. The most extensive hot spots were distributed in the Guangming district of Shenzhen (the northwest region), which is dominated economically by the manufacturing industry. Substantial amounts of land in Guangming were newly developed areas in 2011, resulting in intensive urban heat. The highest LST occurred in the cargo terminal and bonded areas of Qianhai Bay in southwestern Shenzhen. Additionally, although higher LSTs existed in Guangzhou, the number of pixels with higher LSTs was larger in Shenzhen, as displayed in the violin plots of the LST in Fig. 3c.

Representative landscape metrics detection

Note that we defined the maximum number of landscape metrics in the subsets to be 10. The number of influencing landscape metrics actually extracted by the stepwise regression was greater than 10 for both cities. The results indicated that the achieved accuracies of the LST prediction increased as the number of landscape metrics included in the models increased (Fig. 4). The results demonstrated that the explanation rates increased greatly with the increase in the number of landscape metrics from one to four (Fig. 4). The explanation rate with only one landscape metric (PER) exhibited the lowest explanation rates of 70.72% and 77.18%, and then increased greatly to 73.82% and 78.32% with two landscape metrics (PER and NP) for Guangzhou and Shenzhen, respectively (Table 2). However, these upward tendencies became less steep after the selection of the two landscape metrics. Especially when the number was greater than four, the inclusion of more landscape metrics in the models did not yield significantly higher accuracies. Taking Shenzhen as an example, the explanation rate increased only by 0.07% with an increase in the number of landscape metrics from four to five, with SHAPE_MN (mean of shape index) included as an

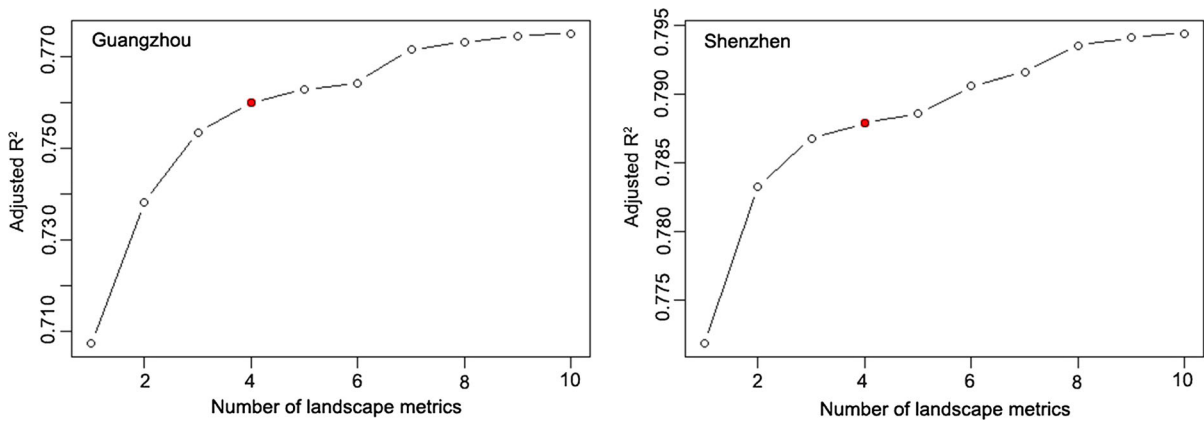


Fig. 4 Adjusted R² changes among different numbers of landscape metrics in the LST prediction models

Table 2 The representative landscape metrics corresponding to the required number of metrics to predict the LST in Guangzhou and Shenzhen

Number of metrics	Representative landscape metrics selection							
1	<u>PER</u>							
2	<u>PER</u>	<u>NP</u>						
3	<u>PER</u>	<u>NP</u>	FRAC_AM					
4	<u>PER</u>	<u>NP</u>	FRAC_AM	AREA_AM				
			AREA_AM	CIRCLE_MN				
5	<u>PER</u>	<u>NP</u>	FRAC_AM	AREA_AM	TE			
			AREA_AM	CIRCLE_MN	SHAPE_MN			
6	<u>PER</u>	<u>NP</u>	FRAC_AM	AREA_AM	TE	SHAPE_AM		
			AREA_AM	CIRCLE_MN	SHAPE_MN	GYRATE_MN		
7	<u>PER</u>	<u>NP</u>	FRAC_AM	AREA_AM	TE	SHAPE_AM	GYRATE_AM	
			AREA_AM	CIRCLE_MN	SHAPE_MN	GYRATE_MN	COHESION	

PER percent cover, NP number of patches, AREA_AM area-weighted mean of the patch area, FRAC_AM area-weighted mean of the perimeter-area fractal dimension, CIRCLE_MN mean of the related circumscribing circle, TE total edge, SHAPE_MN mean of the shape index, SHAPE_AM area-weighted mean of the shape index, GYRATE_AM area-weighted mean of the radius of gyration, GYRATE_MN mean of the radius of gyration, and COHESION patch cohesion index. Detailed definitions and equations can be found in the user manual of the Fragstats 4.2 software (McGarigal et al. 2012)

PER and NP with an underline are the same representative landscape metric selections according to the required number for both cities. The landscape metrics with normal font and bold are the selections for Guangzhou and Shenzhen, respectively

added predictor variable with PER, NP, AREA_AM (area-weighted mean of patch area), and CIRCLE_MN (mean of related circumscribing circle) in the model. Similar results could also be found in Guangzhou; hence, we determined that the optimal number of representative landscape metrics is four.

As shown in Table 2, Guangzhou and Shenzhen shared the same representative landscape metrics when we required only one or two landscape metrics

of greenspaces in the LST predicted models, with PER for the first landscape metric selection and an added NP as the second landscape metric. However, these selections for the other numbers of required metrics were different between Guangzhou and Shenzhen. For instance, FRAC_AM (area-weighted mean of fractal dimension index) was the third selection for Guangzhou, whereas AREA_AM was for Shenzhen. In contrast, AREA_AM was the fourth selection of

Guangzhou, but CIRCLE_MN was for Shenzhen. Finally, four specific landscape metrics could be confirmed, as denoted by the gray region in Table 2: PER, NP, FRAC_AM, and AREA_AM for Guangzhou and PER, NP, AREA_AM, and CIRCLE_MN for Shenzhen.

Figure 5 reveals that the Pearson correlation coefficients were considerably high for all four representative landscape metrics, suggesting the existence of significant relationships between the LST and the selected landscape metrics. In detail, the PER and AREA_AM have a slight linear relationship with the LST. The NP was logarithmically related to the LST, with 20 patches of greenspace approximately equaling the threshold value of this relationship. The LST significantly increased as the NP increased before 20 patches in the 500 m × 500 m block, whereas the increase in the greenspace NP did not significantly increase the LST after the threshold for the two cities. The relationship between the FRAC_AM and LST in Guangzhou formed a “crying” concentric curve with the lowest correlation coefficient of 0.40 among all selected landscape metrics.

The CIRCLE_MN serves as a shape metric that measures the circularity and elongation of the patches, it approaches 0 for circular greenspace patches and approaches 1 for elongation. Results showed CIRCLE_MN strongly nonlinearly and positively related to the LST in Shenzhen. A highly convoluted but narrow patch of greenspace may indicate increasing total edges and higher edge density, which would potentially lead to an increase of shade provided by greenspace to surrounding areas (Zhou et al. 2011). To our knowledge, the CIRCLE has been ignored in previous UHI research. However, we found that the CIRCLE is also a valuable metric of greenspace for Shenzhen based on the representative landscape metrics detection procedure.

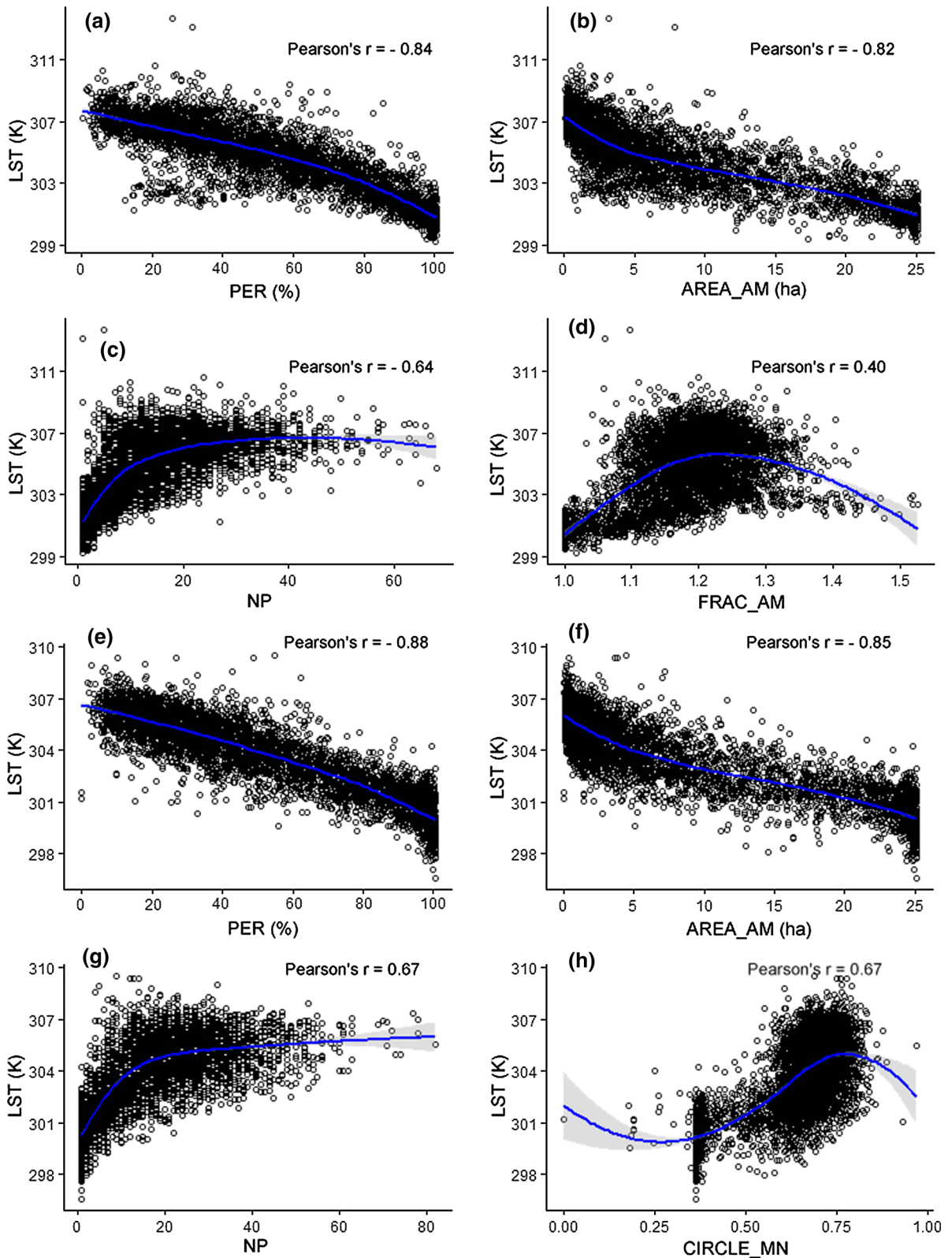
Dominant landscape metrics assessment across the urban landscape

The results indicated that the LST was spatially controlled by the PER, NP, FRAC_AM, and AREA_AM of the greenspace in Guangzhou (Fig. 6a) and by the PER, NP, AREA_AM, and CIRCLE_MN of the greenspace in Shenzhen (Fig. 7a). This suggests that the effect of the greenspace spatial pattern on the LST was dependent on the specific location of the

greenspace. The results revealed that the LST in both cities was dominated by the PER of the greenspace, which accounted for the majority of the blocks compared with the other three landscape metrics—66.93% (or 2902 blocks) for Guangzhou and 64.04% (or 2837 blocks) for Shenzhen. The NP of the greenspace was the next metric, accounting for 13.81% (or 599 blocks) for Guangzhou and 15.62% (or 692 blocks) for Shenzhen. The AREA_AM for Guangzhou and Shenzhen, FRAC_AM for Guangzhou, and CIRCLE_MN for Shenzhen covered relatively fewer blocks.

In addition to confirming that each dominant landscape metric varied across the urban regions, the independent contribution of each block across the study areas was also significantly and spatially heterogeneous (Figs. 6b, 7b). Guangzhou produced higher independent contributions by the dominant landscape metrics, ranging from 7.30 to 66.06%, with a mean of 28.60%, and Shenzhen produced independent contributions ranging from 3.67 to 61.26%, with a mean of 26.96%. It is significant that there were very few blocks that exhibited independent contributions higher than 50%, suggesting that joint contributions interacting with various landscape metrics of greenspaces may be the predominant influencing factor for LST variations.

The IDG that determines the magnitude of the dominance difference of each selected landscape metric is shown in Fig. 8. In particular, we classified the blocks with a IDG less than 10% as weak magnitude, blocks with a IDG greater than 10% and less than 20% as strong magnitude, and blocks with a IDG greater than 20% as very strong magnitude. The results suggested that a larger number of blocks in the two cities were covered by weak and strong magnitudes. In detail, 2026 (or 47.80%) and 2048 (or 47.23%) blocks in Guangzhou were weak and strong, respectively. These numbers were 2623 (59.21%) and 1708 (38.55%) blocks for Shenzhen. The PER accounted for the greatest number of blocks, especially those of strong magnitude in Guangzhou (1568 blocks) and weak magnitude in Shenzhen (1469 blocks), which is reasonable because the PER of greenspace covered most of the blocks in the two cities. It is interesting to note that the AREA_AM, rather than the NP, covered the second most number of blocks, following the PER with weak magnitudes, indicating that most of the AREA_AM blocks



◀ **Fig. 5** Scatterplots showing the relationships between the LST and the selected landscape metrics of Guangzhou (a–d) and Shenzhen (e–h). All the correlation coefficients were significant at the 0.01 level. The trend lines fitting the scatterplots were based on a loess smoother

exhibited a weaker dominant ability in determining the LST compared with the other landscape metrics. Only a small number of blocks exhibited a very strong magnitude. In these cases, the PER accounted for 244 blocks for Guangzhou and 66 blocks for Shenzhen. The NP followed, accounting for 11 and 22 for

Guangzhou and Shenzhen, respectively. The other landscape metrics exhibited fewer than 10 blocks.

Discussion

Representative landscape metrics selection

Numerous landscape metrics have been used to derive the LST in various studies (Zhou et al. 2011, 2017b; Peng et al. 2018; Liu et al. 2018b; Guo et al. 2019; Li and Zhou 2019; Yue et al. 2019). However, most of these studies tended to subjectively select several

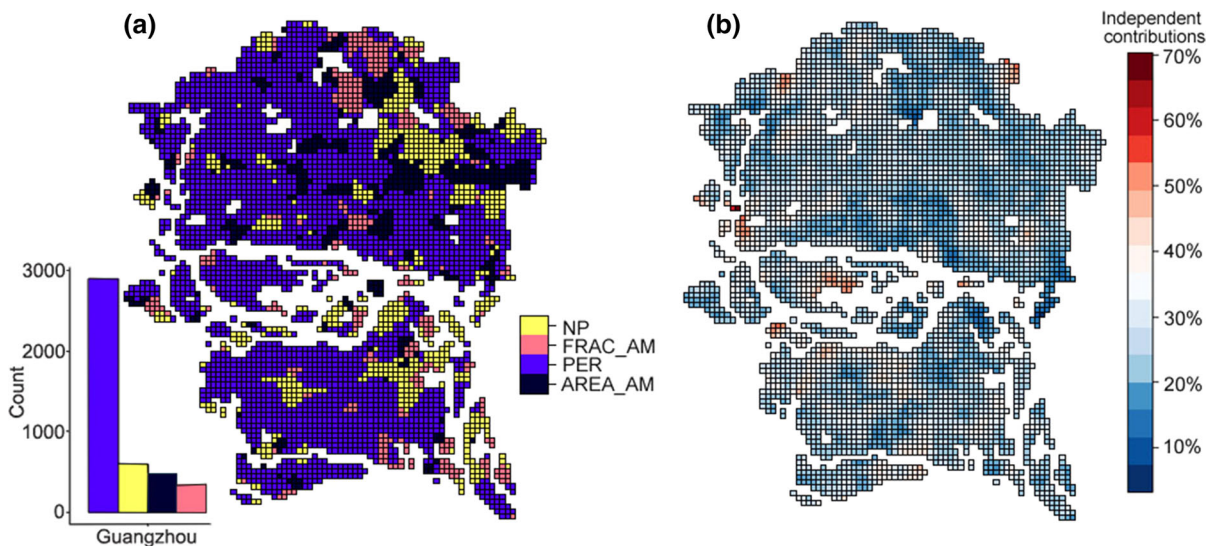


Fig. 6 a Spatial distribution of each dominant landscape metric and b their independent contributions in Guangzhou

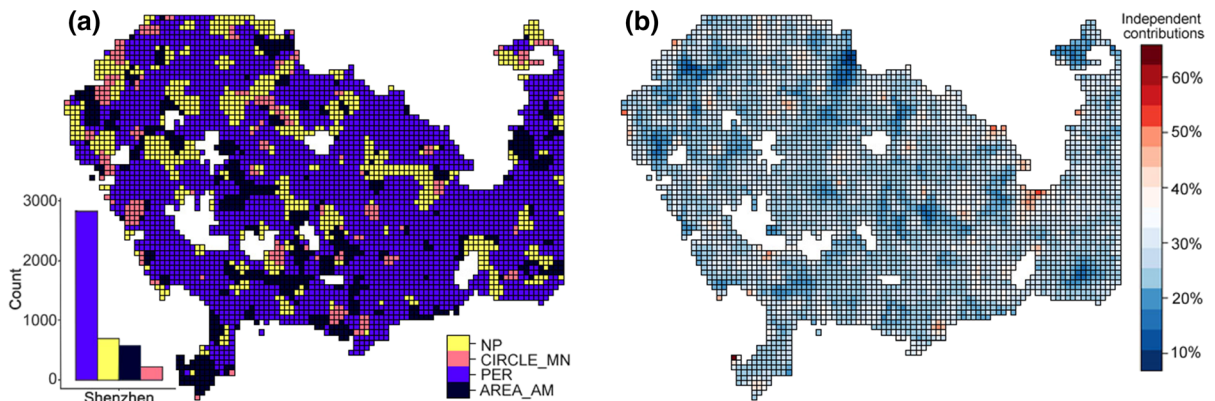


Fig. 7 a Spatial distribution of each dominant landscape metric and b their independent contributions in Shenzhen

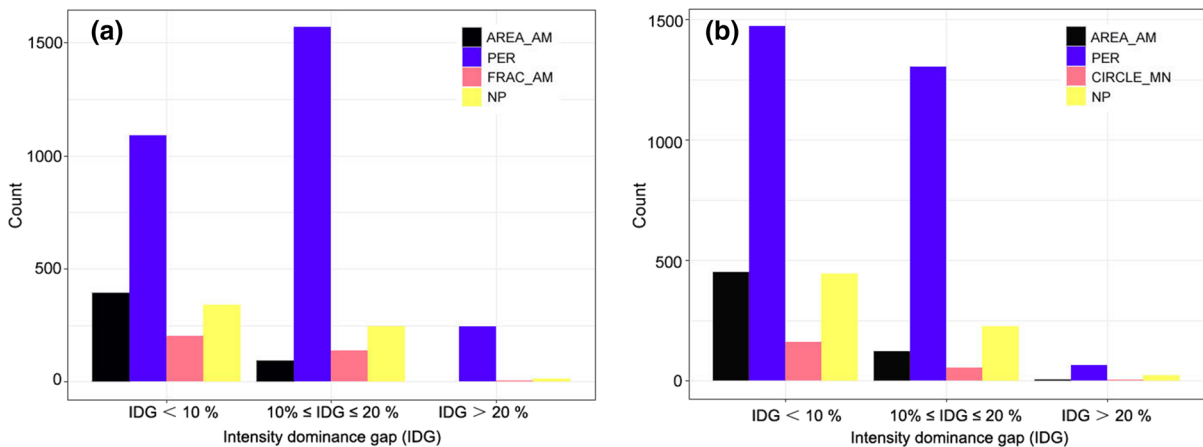


Fig. 8 Intensity dominance gap (IDG) of each landscape metric for **a** Guangzhou and **b** Shenzhen. Note that a IDG less than 10% was defined as weak magnitude, IDG greater than 10% and less

than 20% was defined as strong magnitude, and IDG greater than 20% was defined as very strong magnitude

commonly used metrics according to previous efforts. In this study, we found it vital to reduce the number of landscape metrics and select the most representative and significant landscape metrics of greenspaces because the LST was found to vary dramatically across the study areas, and its value is strongly dependent on the background climate and urban planning (Zhou et al. 2017b, 2018; Guo et al. 2019).

Focusing on the different behaviors of the various landscape metrics of greenspaces to explain the LST, we took Guangzhou and Shenzhen as the study areas to test the proposed method and conduct comparative work. We found the PER, NP, and AREA_AM to be representative landscape metrics for both cities when three landscape metrics were required to predict the LST (Table 2), even though these two cities were characterized by significantly different LST patterns and socio-economic development backgrounds. Three landscape metrics accounted for more than 75% of the explanation rate in predicting the LST variations. This may be due to the similarity in urban climate or, at least partially, the similarities in the phenological characteristics of greenspaces. These results may help us to confirm that a smaller difference between the study areas means that the representative landscape metrics in deriving the LST are more stable. Additionally, the FRAC_MN and CIRCLE_MN of the greenspace were the other representative landscape metrics. However, these added landscape metrics only yielded a slight improvement in predicting the LST

(Fig. 4), which was consistent with the results of Chen et al. (2014) and Peng et al. (2018).

The representative landscape metrics found in this study can also be seen clearly through comparisons with previous efforts. For example, Zhou et al. (2017b) chose five landscape metrics of urban trees based on various criteria, including theory, practice, easy interpretability, and minimal redundancy (Peng et al. 2010; Zhou et al. 2011; Li et al. 2013), to examine the impacts of spatial patterns of trees on urban heat mitigation in Maryland and California in the USA. Their landscape metrics selection consisted of the PER representing the spatial composition metric and the AREA_MN, ED, SHAPE_MN, and LPI representing the spatial configuration metrics. Li and Zhou (2019) chose similar landscape metrics as stated by Zhou et al. (2017b), replacing the AREA_MN with the PD to investigate the relationship between the urban heat island and greenspace spatial pattern in the Illinois–Indiana–Ohio urban agglomeration in the USA. Guo et al. (2019) selected the PER, MPS, ED, and LPI based on previous work (Cushman et al. 2008) to examine the complex mechanisms linking the LST to the greenspace spatial pattern in four highly urbanized cities in China. It is clear that these efforts improved our understanding of the mechanisms of the LST. However, regarding the significantly different locations of the corresponding study areas worldwide, the potential driving factors and underlying mechanisms of the LST might differ.

Although the selected metrics predicting the LST exhibit significant variances, the subjective landscape metrics selection probably leads to multi-collinearity among the predictors or over-fitting of the model (Asgarian et al. 2015; Peng et al. 2018; Rocha et al. 2019). These problems can be overcome by reducing the number of independent variables prior to investigating the associations with the independent and dependent variables using appropriate statistical techniques (Riitters et al. 1995; Dohoo et al. 1997; Chen et al. 2014). Consequently, the representative landscape metrics selection approach proposed in this study is more reasonable. Our results demonstrate explicitly that the landscape metrics selection was a site-specific task, stressing the importance of quantitatively identifying the best independent variables during the research on the relevant physical mechanisms. Moreover, the idea of a representative landscape metrics selection approach can also be broadly applied to research on other environmental and ecological mechanisms.

Site-specific mechanism for UHI management implication

In this study, we developed a spatially explicit approach, joining the GWR and hierarchical partitioning analysis, to characterize and map the dominant landscape metrics locally across Guangzhou and Shenzhen. Beyond the non-stationary mechanism of the LST with the use of the GWR, as revealed in previous studies (Li et al. 2010; Ivajnsič et al. 2014; Zhang et al. 2019), we further detected the dominant landscape metric of the greenspace spatially and locally based on the local R^2 results derived from the GWR model (Figs. 6, 7). Based on this approach, we could effectively detail the spatial distribution of the dominant landscape metric of the greenspace in a study area with block scale and, thus, improve our understanding of the specific metric that determines the LST locally. This method also allows us to spatially detail the magnitude of the dominant ability of each dominant landscape metric (Fig. 8). This issue is vital because if the dominant intensity of the most powerful landscape metric of greenspace was weak, we would have to consider the second most powerful landscape metric when managing and planning a greenspace to implement UHI mitigation strategies.

Unlike global statistical methods, which only provide an average description of the LST mechanism over all sites, our proposed method can provide more detailed local information regarding how the spatial variations of the LST were affected by the greenspace spatial patterns in blocks. The information from these local sites is helpful in implementing more target-specific and effective greenspace planting strategies to decrease the LST and mitigate the UHI. For example, we found that the greenspace composition was not always the most significant landscape metric influencing the LST variations, as found in previous studies based on global statistical methods. Our study confirmed that the greenspace composition is the dominant influencing metric, but not across all sites of the cities. The greenspace configuration (e.g., AREA_AM) tended to have a much stronger impact on the LST than the greenspace composition in some local sites (Fig. 8), where we can focus on optimizing the greenspace configuration with a limited greenspace area.

Many cities in China have recently begun implementing the “Urban Green Space System Planning” policy to improve the ecosystem services of greenspaces. The results of our study are beneficial for these implementations because when cities have limited land available for greening, urban planners can consider opportunities for optimizing greenspace configurations for fixed areas to further alleviate the UHI in these areas, rather than only seeking sufficiently large areas for planting new greenspaces. The regional differentiation of the dominant landscape metrics will serve to provide specific UHI mitigation strategies toward practical implementations, rather than a “one-size-fits-all” policy (Platt 2004), allowing urban planners and designers to lead the way in UHI mitigation, urban resilience, and sustainable development.

Limitations and future work

The method proposed in this study provides a potentially valuable idea for investigating the complex relationship between the LST and greenspace patterns; however, all the results should be interpreted in the context of several limitations. First, a single statistical scale (500 m × 500 m) was used in this study, regardless of the spatial dependence of the LST-deriving influence relationship (Zhou et al. 2017b; Liu

et al. 2018b; Guo et al. 2019). The greenspace and its cooling effect may transcend far from its physical boundary (Zhou et al. 2015). Future research should consider a multi-scale analysis and neighborhood information within the blocks. Next, this study only considered the landscape metrics of greenspaces. The surface albedo, water body, urban morphology, and other important physical and socioeconomic properties were not fully analyzed as LST-influencing factors. Thus, targeting the specific government department adopting relevant scientific findings to guide the selection of the LST-influencing factors in a certain study area is a desirable process in future studies. In addition, we assumed that the LST derived from a single Landsat image could provide a representative urban heat condition during a summer daytime in the subtropics. However, the daytime temperature in the urban area reaches its peak in the summer afternoon (Wong et al. 2016), whereas the Landsat images record the LST at approximately 10:45 am (local time). Considering the lack of a satellite-based remote sensing image revealing the LST in the afternoon, the LST information combined with temperature field measurements of land surface and canopy layer in urban areas might be an effective framework for better understanding the mechanism of the UHI.

Conclusion

Quantitatively mapping the dominant landscape metrics of greenspaces to determine the LST is crucial for understanding the local UHI mechanism, facilitating a more holistic understanding of the topological relationships between the greenspace and LST and a flexible implementation of greenspace planning policy for local sites and UHI mitigation. Both the greenspace spatial patterns and LST in urban sites were highly heterogeneous. Urban planners and designers frequently seek spatially explicit tools to make strategic decisions based on the specific characteristics of urban areas.

In this study, we proposed a new method for mapping and detailing the dominant landscape metrics of greenspaces that locally influence the LST across two selected study areas. The following results were found: (1) the four representative landscape metrics of greenspaces identified from the proposed method

could be used to describe the major LST variations (75.99% with PER, NP, FRAC_AM, and AREA_AM for Guangzhou and 78.79% with PER, NP, CIRCLE_MN, and AREA_AM for Shenzhen). Adding another landscape metric did not significantly improve the prediction ability of the models; (2) the proposed approach could map the dominant landscape metrics of greenspaces that effectively determine the LST across cities, in contrast to previous studies, which identified only the most important influencing factor for the entire study area; (3) the greenspace composition is the primary influencing metric, accounting for the most blocks of the two cities, followed by the NP and FRAC_AM for Guangzhou and CIRCLE_MN for Shenzhen accounting for the fewest blocks. Additionally, most of the blocks have a dominant intensity of landscape metrics of less than 20% (not a very strong magnitude) in the two cities. This proposed method provides an operational spatially explicit tool grounded for urban planners with a fine scale and a local relationship between the greenspace spatial patterns and LST, facilitating the implementation of UHI mitigation strategies.

Acknowledgements This work was jointly funded by the National Natural Science Foundation of China (42071236), NSFC-Guangdong Joint Foundation Key Project (U1901219) and key Special Project for Introduced Talents Team of Southern Marine Science and Engineering Guangdong Laboratory in Guangzhou, China (GML2019ZD0301).

References

- Arnfield AJ (2003) Two decades of urban climate research: a review of turbulence, exchanges of energy and water, and the urban heat island. *Int J Climatol* 23(1):1–26
- Asgarian A, Amiri BJ, Sakieh Y (2015) Assessing the effect of green cover spatial patterns on urban land surface temperature using landscape metrics approach. *Urban Ecosyst* 18(1):209–222
- Brunsdon C, Fotheringham AS, Charlton ME (1996) Geographically weighted regression: a method for exploring spatial nonstationarity. *Geogr Anal* 28(4):281–298
- Chen A, Yao L, Sun R, Chen L (2014) How many metrics are required to identify the effects of the landscape pattern on land surface temperature? *Ecol Ind* 45:424–433
- Chun B, Guldmann J-M (2018) Impact of greening on the urban heat island: seasonal variations and mitigation strategies. *Comput Environ Urban Syst* 71:165–176
- Cushman SA, McGarigal K, Neel MC (2008) Parsimony in landscape metrics: strength, universality, and consistency. *Ecol Ind* 8(5):691–703

- Dohoo IR, Ducrot C, Fourichon C, Donald A, Hurnik D (1997) An overview of techniques for dealing with large numbers of independent variables in epidemiologic studies. *Prev Vet Med* 29(3):221–239
- Foody GM (2003) Geographical weighting as a further refinement to regression modelling: an example focused on the NDVI–rainfall relationship. *Remote Sens Environ* 88(3):283–293
- Gabriel KMA, Endlicher WR (2011) Urban and rural mortality rates during heat waves in Berlin and Brandenburg, Germany. *Environ Pollut* 159(8):2044–2050
- Greene CS, Kedron PJ (2018) Beyond fractional coverage: a multilevel approach to analyzing the impact of urban tree canopy structure on surface urban heat islands. *Appl Geogr* 95:45–53
- Guo G, Zhou X, Wu Z, Xiao R, Chen Y (2016) Characterizing the impact of urban morphology heterogeneity on land surface temperature in Guangzhou, China. *Environ Modell Softw* 84:427–439
- Guo G, Wu Z, Chen Y (2019) Complex mechanisms linking land surface temperature to greenspace spatial patterns: evidence from four southeastern Chinese cities. *Sci Total Environ* 674:77–87
- Ivajnišič D, Kaligarič M, Žiberna I (2014) Geographically weighted regression of the urban heat island of a small city. *Appl Geogr* 53:341–353
- Li X, Zhou W (2019) Optimizing urban greenspace spatial pattern to mitigate urban heat island effects: extending understanding from local to the city scale. *Urban For Urban Greeng* 41:255–263
- Li S, Zhao Z, Miaomiao X, Wang Y (2010) Investigating spatial non-stationary and scale-dependent relationships between urban surface temperature and environmental factors using geographically weighted regression. *Environ Model Softw* 25(12):1789–1800
- Li X, Zhou W, Ouyang Z, Xu W, Zheng H (2012) Spatial pattern of greenspace affects land surface temperature: evidence from the heavily urbanized Beijing metropolitan area, China. *Landsc Ecol* 27(6):887–898
- Li X, Zhou W, Ouyang Z (2013) Relationship between land surface temperature and spatial pattern of greenspace: what are the effects of spatial resolution? *Landsc Urban Plann* 114:1–8
- Li X, Li W, Middel A, Harlan SL, Brazel AJ, Turner BL (2016) Remote sensing of the surface urban heat island and land architecture in Phoenix, Arizona: combined effects of land composition and configuration and cadastral–demographic–economic factors. *Remote Sens Environ* 174(2):233–243
- Liu Y, Peng J, Wang Y (2018a) Application of partial least squares regression in detecting the important landscape indicators determining urban land surface temperature variation. *Landsc Ecol* 33(7):1133–1145
- Liu Y, Peng J, Wang Y (2018b) Efficiency of landscape metrics characterizing urban land surface temperature. *Landsc Urban Plann* 180:36–53
- Mac Nally R (2000) Regression and model-building in conservation biology, biogeography and ecology: the distinction between—and reconciliation of—‘predictive’ and ‘explanatory’ models. *Biodivers Conserv* 9(5):655–671
- Maimaitiyiming M, Ghulam A, Tiyyip T, Pla F, Latorre-Carmona P, Halik Ü, Sawut M, Caetano M (2014) Effects of green space spatial pattern on land surface temperature: implications for sustainable urban planning and climate change adaptation. *ISPRS J Photogramm Remote Sens* 89:59–66
- McGarigal K, Cushman SA and Ene E (2012) FRAGSTATS v4: spatial pattern analysis program for categorical and continuous maps. Computer software program produced by the authors at the University of Massachusetts, Amherst. <http://www.umass.edu/landeco/research/fragstats/fragstats.html>.
- Oke TR (1973) City size and the urban heat island. *Atmos Environ* 7(8):769–779
- Peng J, Wang Y, Zhang Y, Wu J, Li W, Li Y (2010) Evaluating the effectiveness of landscape metrics in quantifying spatial patterns. *Ecol Indic* 10(2):217–223
- Peng J, Tian L, Liu Y, Zhao M, Hu YN, Wu J (2017) Ecosystem services response to urbanization in metropolitan areas: thresholds identification. *Sci Total Environ* 607–608:706–714
- Peng J, Jia J, Liu Y, Li H, Wu J (2018) Seasonal contrast of the dominant factors for spatial distribution of land surface temperature in urban areas. *Remote Sens Environ* 215:255–267
- Pickard BR, Van Berkel D, Petrasova A, Meentemeyer RK (2017) Forecasts of urbanization scenarios reveal trade-offs between landscape change and ecosystem services. *Landsc Ecol* 32(3):617–634
- Pickett STA, Cadenasso ML (1995) Landscape ecology: spatial heterogeneity in ecological systems. *Science* 269(5222):331
- Platt RV (2004) Global and local analysis of fragmentation in a mountain region of Colorado. *Agric Ecosyst Environ* 101(2):207–218
- Qin Z, Karnieli A, Berliner P (2001) A mono-window algorithm for retrieving land surface temperature from Landsat TM data and its application to the Israel–Egypt border region. *Int J Remote Sens* 22(18):3719–3746
- Riitters KH, O’Neill RV, Hunsaker CT, Wickham JD, Yankee DH, Timmins SP, Jones KB, Jackson BL (1995) A factor analysis of landscape pattern and structure metrics. *Landsc Ecol* 10(1):23–39
- Rocha AD, Groen TA, Skidmore AK (2019) Spatially-explicit modelling with support of hyperspectral data can improve prediction of plant traits. *Remote Sens Environ* 231:111200
- Seto KC, Güneralp B, Hutyra LR (2012) Global forecasts of urban expansion to 2030 and direct impacts on biodiversity and carbon pools. *Proc Natl Acad Sci* 109(40):16083
- Skelhorn CP, Levermore G, Lindley SJ (2016) Impacts on cooling energy consumption due to the UHI and vegetation changes in Manchester, UK. *Energy Build* 122:150–159
- Su Y-F, Foody GM, Cheng K-S (2012) Spatial non-stationarity in the relationships between land cover and surface temperature in an urban heat island and its impacts on thermally sensitive populations. *Landsc Urban Plann* 107(2):172–180
- Sun R, Chen L (2017) Effects of green space dynamics on urban heat islands: mitigation and diversification. *Ecosyst Serv* 23:38–46

- Taylor L, Hochuli DF (2017) Defining greenspace: multiple uses across multiple disciplines. *Landsc Urban Plann* 158:25–38
- Turner MG (2005) Landscape ecology: what is the state of the science? *Annu Rev Ecol Evol Syst* 36:319–344
- Van Donkelaar A, Martin RV, Spurr RJD, Burnett RT (2015) High-resolution satellite-derived PM_{2.5} from optimal estimation and geographically weighted regression over North America. *Environ Sci Technol* 49(17):10482–10491
- Voogt JA, Oke TR (2003) Thermal remote sensing of urban climates. *Remote Sens Environ* 86(3):370–384
- Wang X-J (2009) Analysis of problems in urban green space system planning in China. *J For Res* 20(1):79–82
- Wang Q, Zhao P, Ren H, Kakubari Y (2008) Spatiotemporal dynamics of forest net primary production in China over the past two decades. *Glob Planet Change* 61(3–4):267–274
- Wang J, Zhou W, Qian Y, Li W, Han L (2018a) Quantifying and characterizing the dynamics of urban greenspace at the patch level: a new approach using object-based image analysis. *Remote Sens Environ* 204:94–108
- Wang Y, Nordio F, Nairn J, Zanobetti A, Schwartz JD (2018b) Accounting for adaptation and intensity in projecting heat wave-related mortality. *Environ Res* 161:464–471
- Wong PP-Y, Lai P-C, Low C-T, Chen S, Hart M (2016) The impact of environmental and human factors on urban heat and microclimate variability. *Build Environ* 95:199–208
- Wu J, David JL (2002) A spatially explicit hierarchical approach to modeling complex ecological systems: theory and applications. *Ecol Model* 153(1):7–26
- Wu W, Zhao S, Zhu C, Jiang J (2015) A comparative study of urban expansion in Beijing, Tianjin and Shijiazhuang over the past three decades. *Landsc Urban Plann* 134:93–106
- Xu Z, FitzGerald G, Guo Y, Jalaludin B, Tong S (2016) Impact of heatwave on mortality under different heatwave definitions: a systematic review and meta-analysis. *Environ Int* 89–90:193–203
- Yue W, Liu X, Zhou Y, Liu Y (2019) Impacts of urban configuration on urban heat island: an empirical study in China mega-cities. *Sci Total Environ* 671:1036–1046
- Zhang Y, Murray AT, Turner BL (2017) Optimizing green space locations to reduce daytime and nighttime urban heat island effects in Phoenix, Arizona. *Landsc Urban Plann* 165:162–171
- Zhang Y, Middel A, Turner BL (2019) Evaluating the effect of 3D urban form on neighborhood land surface temperature using Google Street View and geographically weighted regression. *Landsc Ecol* 34(3):681–697
- Zhou W, Huang G, Cadenasso ML (2011) Does spatial configuration matter? Understanding the effects of land cover pattern on land surface temperature in urban landscapes. *Landsc Urban Plann* 102(1):54–63
- Zhou D, Zhao S, Zhang L, Sun G, Liu Y (2015) The footprint of urban heat island effect in China. *Sci Rep* 5:11160
- Zhou W, Pickett STA, Cadenasso ML (2017a) Shifting concepts of urban spatial heterogeneity and their implications for sustainability. *Landsc Ecol* 32(1):15–30
- Zhou W, Wang J, Cadenasso ML (2017b) Effects of the spatial configuration of trees on urban heat mitigation: a comparative study. *Remote Sens Environ* 195:1–12
- Zhou D, Bonafoni S, Zhang L, Wang R (2018) Remote sensing of the urban heat island effect in a highly populated urban agglomeration area in East China. *Sci Total Environ* 628–629:415–429
- Zhou W, Fisher B, Pickett STA (2019) Cities are hungry for actionable ecological knowledge. *Front Ecol Environ* 17(3):135–135
- Ziter CD, Pedersen EJ, Kucharik CJ, Turner MG (2019) Scale-dependent interactions between tree canopy cover and impervious surfaces reduce daytime urban heat during summer. *Proc Natl Acad Sci* 116:7575

Publisher's Note Springer Nature remains neutral with regard to jurisdictional claims in published maps and institutional affiliations.